JOURNAL OF COMPUTATIONAL PHYSICS 121, 373–382 (1995)

Orthogonal Collocation in the Nonconforming Boundary Element Method

SRIGANESH R. KARUR AND P. A. RAMACHANDRAN

Department of Chemical Engineering, Washington University, 1 Brookings Drive, Campus Box 1198, St. Louis, Missouri 63130

Received October 5, 1994; revised April 10, 1995

This paper outlines the use of non-conforming (discontinuous) elements in the collocation boundary element method for solving two-dimensional potential and Poisson type problems. The roots of an orthogonal polynomial (shifted Jacobi polynomial) are used as the collocation points. This results in increased accuracy due to the least square minimization property of the orthogonal polynomials. The advantage of using non-conforming elements is realized when the method is applied (i) to problems with singularities (both due to geometry and boundary conditions) and (ii) in conjunction with domain decomposition techniques. Also, the collocation points can be relocated within an element by changing two user-defined parameters in the shifted Jacobi polynomial, thus providing an error indicator which can be used for mesh refinement purposes. This technique, called the *rh* method, is discussed and illustrated. The results obtained by using non-conforming boundary elements for standard test problems are shown to be accurate.

1. INTRODUCTION

The boundary element method (BEM) is a powerful numerical tool used for solving linear elliptical partial differential equations [1, 2] since the dimensionality of such problems is reduced by one. For example, a 2D/3D object is discretized only along its perimeter/surface. The discretization is done by dividing the perimeter into small segments called boundary elements. The dependent variable is then approximated along each element by placing a certain number of nodes. Depending on the location of the nodes, the boundary elements get classified as conforming (continuous) or non-conforming (discontinuous). Conforming elements are those in which two adjoining elements share a common node. Non-conforming elements are those in which neighboring elements do not share a common node. When using conforming elements in BEM, one has to tackle the problem of singularities which can occur due to the geometry of the domain or due to the imposed boundary conditions. For example, when Dirichlet (D) type boundary condition is specified on two elements intersecting at a sharp corner, the problem becomes underspecified (more number of unknowns than the number of equations) and, hence, the normal gradient at the corner cannot be determined uniquely. Also, when mixed boundary conditions (for example, Dirichlet condition on an element and Neumann condition (N) on its neighboring element) are imposed on a smooth boundary, the normal gradient becomes undefined at the intersection of these two elements. To solve such problems special techniques have to be used to resolve the normal gradient at the singular points in the case of conforming elements [3–5].

The use of non-conforming boundary elements instead of the conforming elements is the easiest way to handle such complexities. The chief advantage in using such elements is that the singularities arising due to geometry and boundary conditions can be avoided without compromising on the accuracy of the solution as illustrated in this work. A criticism for using non-conforming elements is that the potential is discontinuous at the intersection of two elements. By placing the collocation points close enough to the element end points and at optimal locations as shown in this work, this error can be minimized. The use of non-conforming elements is fully realized when BEM is applied along with domain decomposition techniques. Domain partitioning is necessary in handling situations where the governing differential equation varies in each sub-region. For instance if a domain is split into four sub-domains, careful bookkeeping is necessary to implement the compatibility conditions especially at the node corresponding to the point of intersection of all the four domains. By using non-conforming elements, this node can effectively be eliminated from the computation without sacrificing on the accuracy of the solution. Hence, the use of non-conforming elements in BEM offers some distinct advantages over conforming elements.

The piecewise constant approximation (constant elements) which belongs to the class of non-conforming elements is widely being used in the literature [1, 6, 7]. Some researchers have used higher order non-conforming elements to solve elastostatics [8, 9] and electromagnetic problems [10]. However, these works do not provide a concrete strategy for the placement of the collocation points within an element. The accuracy of BEM strongly depends on the choice of the collocation points. An optimal choice would enable one to validate the usefulness of non-conforming elements in several new application areas. In this study, a rational choice for the placement of the collocation

0021-9991/95 $12.00

points within an element is provided. This is the first highlight of the paper. The roots of an orthogonal polynomial (the shifted Jacobi polynomial) are used as the collocation points. The provision to generate several sets of collocation points by changing two user defined parameters is the major advantage in using the shifted Jacobi polynomial. Flexibility to vary the collocation points while still maintaining orthogonality is provided by this choice. The implementation of this new feature for identifying the discretization error, which has not been addressed before, is the second highlight of this work. This technique is known as the *rh* method [11] and is useful in determining the discretization error and subsequent mesh refinement. The *rh* method developed here is based on heuristic arguments and the technique is demonstrated to be useful but cannot be generalized due to the lack of theoretical basis. By changing the order of the Jacobi polynomial, the number of collocation points can also be changed in an element which is similar to the *p* adaptive technique extensively used in the context of finite element analysis [12].

In this paper, the non-conforming BEM is implemented for the Laplace and linear Poisson type equations. For non-linear Poisson type equations, non-conforming elements can be used in conjunction with the dual reciprocity method (DRM) [13] (closely related to the method of particular integrals). A brief description of BEM and DRM is presented in Section 2. The difference in conforming and non-conforming elements and the choice of collocation points is covered in Section 3. The *rh* method is explained in Section 4. A few illustrative examples are presented in Sections 5, 6, and 7. It is shown numerically, that the results obtained by this method are very accurate for problems in both single and multiple domains. Concluding remarks are provided in Section 8.

2. BOUNDARY ELEMENT METHOD

The main idea behind the BEM is to convert the governing differential equation to an equivalent integral equation. The details of the method can be found in [1, 2, 7, 14]. Consider the Laplace equation,

$$\nabla^2 T = 0, \tag{1}$$

where ∇^2 denotes the Laplacian and T the dependent variable. By applying the Green–Gauss theorem and collocating at the source point i, Eq. (1) can be expressed as the integral equation,

$$\int_\Gamma \left(G \frac{\partial T}{\partial n} - T \frac{\partial G}{\partial n} \right) d\Gamma - d_i T_i = 0, \tag{2}$$

where d_i is a coefficient which depends on the location of the source point i on the boundary, Γ is the boundary of the object and n is the outward normal direction. This is the collocation representation of the BEM, where i is also called as the collocation point. In Eq. (2), G is the fundamental solution for the Laplace equation given by

$$G = -\frac{1}{2\pi} \ln(r), \tag{3}$$

where r is the distance between the source (ξ_1, ξ_2) and the field (x_1, x_2) points and is given by

$$r = \sqrt{(x_1 - \xi_1)^2 + (x_2 - \xi_2)^2}. \tag{4}$$

The boundary conditions can be of the Dirichlet type (T is specified), Neumann type ($\mathrm{d}T/\mathrm{d}n$ is specified) or Robin type (combination of both). Equation (2) can be solved by discretizing the boundary into small elements and assigning a particular variation of the dependent variable on each element. The resulting integrals are evaluated numerically by using a 10-point Gaussian quadrature, which in most of the cases is sufficiently accurate. The discretization results in a system of linear equations which can be solved for the boundary unknowns by using a routine equation solver.

For Poisson type equations the treatment is slightly different. Consider the generalized Poisson type equation,

$$\nabla^2 T = b, \tag{5}$$

where b is called the forcing function, which can be a constant or a function of spatial variables and/or the dependent variable, T. When the Green–Gauss theorem is applied to Eq. (5), a domain integral corresponding to the forcing function still remains in the integral formulation. Thus the RHS of Eq. (2) is no longer zero but given by

$$\mathrm{RHS} = \int_\Omega Gb \, \mathrm{d}\Omega, \tag{6}$$

where Ω is the domain under consideration. There are several ways to handle this domain integral. Of them, the dual reciprocity method (DRM) [15] is the most popular technique. In DRM, the domain integral is transferred to an equivalent boundary integral by approximating the forcing function b over the entire domain using suitable basis functions. For this purpose, certain number of internal nodes are required along with the usual number of boundary nodes as in regular BEM. The details of the method are not discussed here for brevity and can be readily found in [15, 16].

In this work, we also consider a Poisson type equation of the diffusion–reaction type, i.e.,

$$\nabla^2 c = \phi^2 c^n, \tag{7}$$

where c is the concentration of the diffusing species, ϕ is a parameter proportional to the ratio of the reaction rate constant to the diffusion coefficient, and n is the order of the reaction.

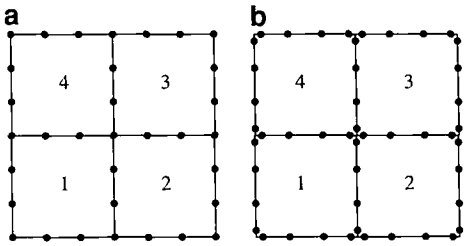

FIG. 1. Difference in node location for conforming and nonconforming (cubic) elements in domain decomposition.

For linear problems, i.e., $n = 1$, the use of special fundamental solution of the form

$$G_{dr} = \frac{1}{2\pi} K_0(\sqrt{\phi} r) \tag{8}$$

reduces the problem to boundary only formulation [17]; i.e., the problem can be solved by regular BEM without any internal nodes. We use this technique for case study 3 in Section 5. For non-linear problems, i.e., $n \neq 1$, the DRM is used to solve the diffusion–reaction equation as illustrated in Section 7.

If the governing partial differential equations vary from region to region in a given domain, then it is necessary to use subdomain (domain decomposition) techniques. A typical situation arises in solving the heat conduction problem with variable thermal conductivity in different regions of the domain. Another example occurs in solving the diffusion reaction equation in a porous catalyst particle, where a Poisson type equation is applicable in the region containing active catalyst and the Laplace equation is applicable in the inert region. In such situations, the domain is partitioned into sub-regions and the BEM is applied to each of these regions separately.

The handling of the variables at the interfacial nodes is crucial in such problems and the use of non-conforming elements reduces the amount of bookkeeping considerably. For instance, the resolution of the normal gradient at the intersection of more than two subdomains poses a problem when conforming elements are used. Figure 1 shows the difference in discretization by using conforming and non-conforming elements when a domain is divided into four subregions. An example to illustrate the use of non-conforming BEM in solving the Laplace equation in multiple domains is presented in Section 5 as part of the case studies.

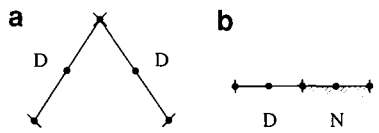

FIG. 3. Singularities due to (a) geometry and (b) boundary conditions.

3. TYPES OF ELEMENTS

Depending upon the nature of approximation, the boundary elements acquire the name of constant, linear, quadratic, cubic element, etc. Figure 2 shows typical higher order conforming elements with the above-mentioned variation of the dependent variable over the length of the element. In many practical cases higher order elements are often used to accurately represent (i) a curved boundary and (ii) the variation of the dependent variable over an element. In conforming elements, the collocation points are necessarily placed at the element end points. This acts to the disadvantage of the conforming elements as the singularities resulting from the geometry and the boundary conditions essentially leave the normal gradient unresolved at those points. Figure 3 shows two such situations.

Figure 3a shows a case of singularity due to the intersection of two elements with Dirichlet boundary condition at a sharp corner. This situation is called the D-D singularity, where the normal gradient is not uniquely defined at the point of singularity. Figure 3b shows a case of singularity arising due to the imposition of Dirichlet boundary condition on one element and Neumann boundary condition on the next element. This is called the D-N singularity and the normal gradient does not exist at the point of singularity. Usually special techniques are needed to handle such singularities when conforming elements are used.

The use of non-conforming elements offers a simple solution to overcome these difficulties. Figure 4 shows the node placement for such elements. The choice of the location of the nodes which is an important feature of this paper is presented in the following sub-section. The manner in which the singularities are avoided by using non-conforming elements is illustrated in Figs. 5a and b.

3.1. *Choice of Collocation Points*

A rational choice for placing the collocation points in non-conforming elements is not available in the literature. Villadsen and Michelsen [18] discuss the basics of collocation methods

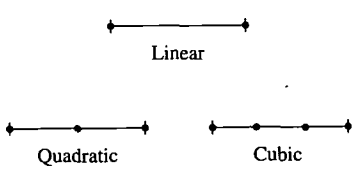

FIG. 2. Examples of conforming elements.

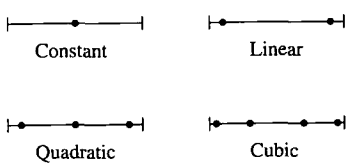

FIG. 4. Examples of non-conforming elements.

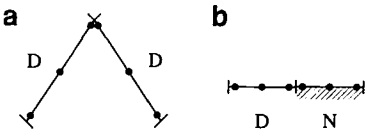

FIG. 5. Handling of singularities by non-conforming elements.

as applicable to ordinary differential equations. They point out that when the collocation points are optimally placed in an interval, the performance of the collocation method is equal to or better than other weighted residual techniques. Since the roots of an orthogonal polynomial are chosen as the collocation points, they call the method an orthogonal collocation. The orthogonal expansion of a given function minimizes the mean square error when the series is terminated after a finite number of terms [19]. Mathematically, if $g(x)$ is the function being interpolated by a set of polynomials $\phi_i(x)$ of degree n, then the least square error defined over an interval $[a, b]$ as

$$\int_a^b W(x)\left(g(x) - \sum_{i=0}^{n} c_i \phi_i(x)\right)^2 \mathrm{d}x \tag{9}$$

is a minimum only if $\phi_i(x)$ are orthogonal to each other with respect to the weighing function $W(x)$. Here c_i are the coefficients of the appropriate orthogonal expansion of $g(x)$ in terms of $\phi_i(x)$. In Eq. (9), n denotes the order of the polynomial (i.e., $n + 1$ collocation points). When the limits of integration, a and b, are taken to be 0 and 1, respectively, and the polynomials $\phi_i(x)$ are orthogonal with respect to $W(x) = 1$, then $\phi_i(x)$ are called shifted Legendre polynomials. For those cases when $\phi_i(x)$ are orthogonal with respect to $W(x) = x^\beta(1 - x)^\alpha$ (where $0 \le x \le 1$ and $\alpha, \beta > -1$), they are called shifted Jacobi polynomials. Notice that Legendre polynomials are a special case of Jacobi polynomials, when $(\alpha, \beta) = (0, 0)$.

In this work, the roots of the shifted Jacobi polynomials, $P_{n+1}^{(\alpha,\beta)}(x)$ are chosen as the collocation points on an element in BEM and, therefore, the current procedure can be called the orthogonal collocation BEM. Consider the expansion of the dependent variable in terms of shifted Jacobi polynomials as

$$\begin{aligned} T = {} & c_0 P_0^{(\alpha,\beta)}(x) + c_1 P_1^{(\alpha,\beta)}(x) + c_2 P_2^{(\alpha,\beta)}(x) \\ & + c_3 P_3^{(\alpha,\beta)}(x) + c_4 P_4^{(\alpha,\beta)}(x) + \cdots . \end{aligned} \tag{10}$$

For a cubic approximation of T, the series in the RHS of Eq. (10) is truncated after the first four terms. The truncation error introduced is then the term corresponding to $P_4^{(\alpha,\beta)}(x)$. This error can be forced to zero at four points in the interval by setting the collocation points as the roots of $P_4^{(\alpha,\beta)}(x) = 0$. This provides for a superconvergence at the collocation points since the truncation error is zero at these points. Hence the truncated version of Eq. (10) is the "best" cubic approximation to the dependent variable. Also, by changing the parameters (α, β), different sets of orthogonal polynomials (hence, different sets of collocation points) can be generated. This can further be used fruitfully in the *a posteriori* error estimation studies.

The polynomials, $P_n^{(\alpha,\beta)}(x)$, can be generated by using the Rodrigues' formula (see, for example, [20, 21]),

$$\begin{aligned} (1 - x)^\alpha x^\beta P_n^{(\alpha,\beta)}(x) = {} & (-1)^n \frac{\Gamma(\beta + 1)}{\Gamma(n + \beta + 1)} \frac{d^n}{dx^n} \\ & \times [(1 - x)^{n+\alpha} x^{n+\alpha}], \end{aligned} \tag{11}$$

where Γ is the gamma function and n is the order of the polynomial. Table I shows the roots of the shifted Jacobi polynomial of order 4 for different combinations of α and β.

By varying the values of α and β, the roots (and, hence, the collocation points) can be weighted towards either one or the other end of the element. As observed from Table I, different values of α and β give different node locations in the normalized interval (0, 1). For example, for $\alpha = 0$ and $\beta = 4$, the nodes are placed close to $x = 1$. But for $\alpha = \beta = 4$, the first and the last nodes are placed away from the two end points, whereas for $\alpha = \beta = -0.5$ they are placed close to the end points. In this study, $(\alpha, \beta) = (0, 0)$ is used for placing the collocation points and we call this the base case. Changing (α, β) from (0, 0) to say (1, 1), yields another set of collocation nodes. Comparison between the solutions obtained from the node configuration resulting from these two sets of (α, β) provides with an error indicator for each element as shown in the next section.

3.2. *Interpolating Functions*

The interpolating functions used to approximate the dependent variable for each element is represented by the Lagrangian form. We use cubic elements for all our computation because they represent the variation of the dependent variables more accurately than lower order elements [20]. Isoparametric trans-

TABLE I

Roots of the Shifted Jacobi Polynomial, $P_4^{(\alpha,\beta)}$

α	β	Roots	α	β	Roots
		0.0694			0.0381
0.0	0.0	0.3300	−0.5	−0.5	0.3087
		0.6700			0.6913
		0.9306			0.9619
		0.1175			0.2013
1.0	1.0	0.3574	4.0	4.0	0.3962
		0.6426			0.6038
		0.8825			0.7987
		0.3121			0.0373
0.0	4.0	0.5789	4.0	0.0	0.1871
		0.8129			0.4211
		0.9627			0.6879

formation is used to relate the positional variable in the actual domain to the standard domain (η coordinate system, where η is the dimensionless arc length). The Lagrangian form of the interpolation functions for cubic elements in the standard domain, where $0 \leq \eta \leq 1$, are given by

$$\phi_1 = \frac{(\eta - \eta_2)(\eta - \eta_3)(\eta - \eta_4)}{(\eta_1 - \eta_2)(\eta_1 - \eta_3)(\eta_1 - \eta_4)} \tag{12}$$

$$\phi_2 = \frac{(\eta - \eta_3)(\eta - \eta_4)(\eta - \eta_1)}{(\eta_2 - \eta_3)(\eta_2 - \eta_4)(\eta_2 - \eta_1)} \tag{13}$$

$$\phi_3 = \frac{(\eta - \eta_4)(\eta - \eta_1)(\eta - \eta_2)}{(\eta_3 - \eta_4)(\eta_3 - \eta_1)(\eta_3 - \eta_2)} \tag{14}$$

$$\phi_4 = \frac{(\eta - \eta_1)(\eta - \eta_2)(\eta - \eta_3)}{(\eta_4 - \eta_1)(\eta_4 - \eta_2)(\eta_4 - \eta_3)} \tag{15}$$

where η_1, η_2, η_3, η_4 are the collocation points obtained from the solution of the shifted Jacobi polynomial with $n = 4$, as shown in Table I. The dependent variable is then represented in terms of the interpolating functions as

$$T = \phi_1 T_1 + \phi_2 T_2 + \phi_3 T_3 + \phi_4 T_4, \tag{16}$$

where T_i ($i = 1, 4$) are the values of the dependent variable at the collocation nodes.

In this work, the geometry of an element is approximated in an optimal way (in the least square sense), by using the same isoparametric representation as described for the dependent variable, i.e.,

$$x = \sum_{i=1}^{4} \phi_i x_i \tag{17}$$

$$y = \sum_{i=1}^{4} \phi_i y_i. \tag{18}$$

In describing the geometry of an element, one can use a superparametric representation (six nodes including the element end points), instead of the isoparametric representation given in Eqs. (17) and (18). Such a representation ensures inter-element continuity and, hence, improved accuracy. However, it is shown in Section 5 that the isoparametric representation is sufficiently accurate to describe the element geometry for the kind of discretization used in this work.

With this prescription of the collocation nodes and the interpolation functions, the collocation version of the integral equation (2) is discretized in a traditional manner.

4. THE *rh* METHOD

Theoretical convergence analysis in collocation boundary element method with conforming elements is very limited [23]. For piecewise constant collocation some convergence results are available [24–27]. For higher order elements the convergence analysis is still under active investigation. In this study we use an empirical approach to estimate the discretization error and to use that information for mesh refining purposes.

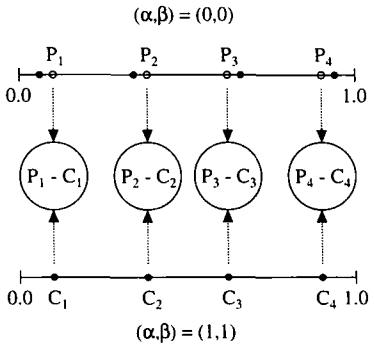

FIG. 6. The *rh* technique: ● are the collocation points and ○ are the projected points for error estimation.

An advantage in using higher order non-conforming elements is that, for the same mesh configuration, different sets of solutions can be generated by changing the two parameters (α, β). The *rh* method uses this concept to get an insight for a possible mesh refinement. In this work, we provide a criteria for the mesh refinement based on an element level error indicator. The error indicator proposed in this work is based on the difference between two solutions obtained by changing the parameters (α, β). For this purpose, we use (α, β) = (0, 0) and (1, 1). The choice of (α, β) is not unique; for example, one can use (-0.5, -0.5) or (2, 2) or any other combination. We use (1, 1) because the collocation points of this combination are not located far away from those of the base case (0, 0). The solution obtained by (α, β) = (0, 0) is used to project solutions at those points which are the collocation points corresponding to (α, β) = (1, 1) as shown in Fig. 6.

This projected solution is compared with the computed solution of (α, β) = (1, 1) in a least square sense. The root mean square (RMS) error, e, is given as

$$e = \sqrt{\left(\frac{1}{4}\sum_{i}^{4} (P_i - C_i)^2\right)} \tag{19}$$

where, P_i and C_i are the projected and the calculated values of the dependent variable at the collocation points corresponding to (α, β) = (1, 1). An indicator of error, ε, for an individual element is defined as

$$\varepsilon = le, \tag{20}$$

where l is the chord length of the element which acts as a weighting parameter. A tolerance limit is set on this indicator, ε, for the refinement process to stop. The method developed here closely follows the concept developed by Guiggiani [11].

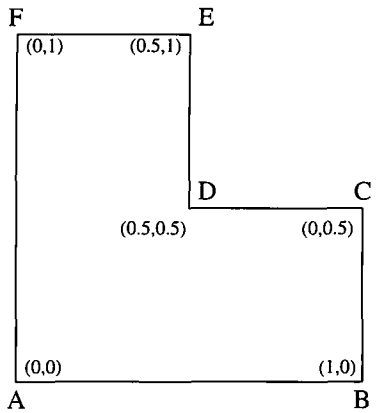

FIG. 7. Geometric singularity; Dirichlet conditions at the boundary means that the normal gradients at the corner nodes are not uniquely defined.

Guiggiani uses conforming quadratic elements with the location of only the center node altered to generate two sets of solutions. The comparison of these two solutions through an L_2 norm provides element level error indicators. However, the relocation of the center node involves some empiricism and Guiggiani also reports non-physical oscillation in the solution when truly non-conforming elements are used. In the present work we use the cubic non-conforming elements with the position of all the four collocation nodes being altered. Again the error is compared in a least square sense. No empirical factors are involved in the choice of collocation nodes and we do not observe any oscillatory behavior in the solution, at least for the class of problems considered here.

5. CASE STUDIES

In this section, some typical examples are provided to demonstrate the performance of the non-conforming elements. The handling of singularities is shown through the comparison of the results with known standards. Laplace and linear diffusion–reaction equations are illustrated in detail since they require discretization along the boundary only. Non-linear problems can be solved similarly by using non-conforming elements in combination with DRM and a brief illustration is presented in Section 7.

Case 1: *Geometric Singularity*

A case of geometric singularity is illustrated here by the study of an *L*-shaped domain with a re-entrant corner (270°), where the normal gradient has no unique value. Figure 7 shows the geometry of the domain. In order to test the use of non-conforming elements a Dirichlet problem with a smooth solution is considered. Thus a harmonic function

$$u = \sin(x)\cosh(y) \tag{21}$$

is used as the Dirichlet boundary conditions so that the numerical solution can be compared with the exact solution. Note that one could have prescribed boundary conditions such that the normal gradient is infinite at the re-entrant corner. We show a similar situation in Case Study 3 when dealing with D-N singularities. For the present example smooth solution is chosen in order to illustrate the treatment for a D-D corner singularity. In the classical BEM special techniques need to be used to resolve the gradient at the corners formed by the intersection of the two elements [7]. In this work, six cubic non-conforming elements (one on each side) are used to discretize the boundary. The normal gradients are calculated along the boundary and a few values are shown in Table II along with the exact solution. The accuracy obtained in the prediction of the normal gradients makes this method very powerful in handling problems with geometric singularities. Note that the discretization is the minimum needed to capture the geometry of the domain. The domain has six sides and only six elements are used. The normal gradients match the analytical solution within roundoff, which is an indication of the effectiveness of this method.

TABLE II

Normal Gradients along *CD* and *DE* for the Dirichlet Problem in an L-Shaped Domain

x	y	Numerical	Analytical
0.9653	0.5000	0.4286	0.4285
0.8350	0.5000	0.3862	0.3863
0.6650	0.5000	0.3214	0.3216
0.5347	0.5000	0.2657	0.2656
0.5000	0.5347	1.0066	1.0061
0.5000	0.6650	1.0790	1.0790
0.5000	0.8350	1.2017	1.2017
0.5000	0.9653	1.3198	1.3192

The normal gradient at the re-entrant corner *D* in Fig. 7 is considered for further study. From the analytical solution the normal gradient tends to 0.25 when approached from *CD* and tends to 1.0 when approached from *ED*. The numerical solution obtained by using six cubic non-conforming elements is extrapolated to get the value of the normal gradient at the point *D*. Table III gives these results for three sets of (α, β). Since all of them give almost the same solution, it is safe to conclude

TABLE III

Value of the Normal Gradient at the D-D Singularity when Approached from *CD* and *ED* for Different Values of (α, β)

From	(0, 0)	(1, 1)	(−0.5, −0.5)	Analytical
CD	0.250	0.249	0.248	0.25
ED	0.990	0.990	0.990	1.00

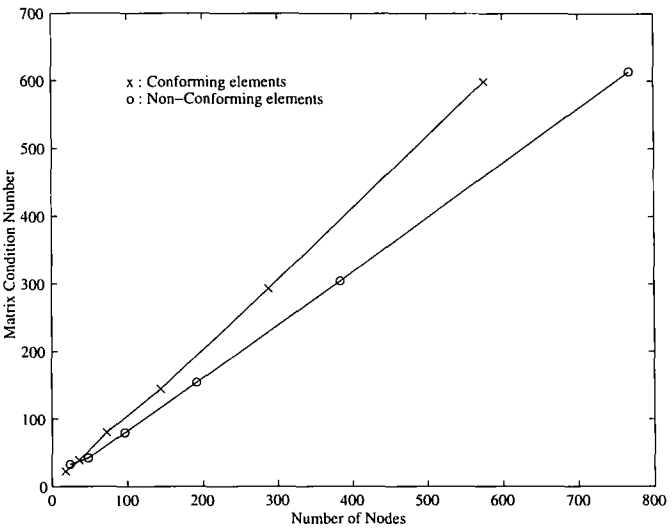

FIG. 8. Condition number of the resultant coefficient matrix for Case 1 using conforming cubic elements (equispaced nodes) and nonconforming cubic elements ($\alpha = \beta = 0$).

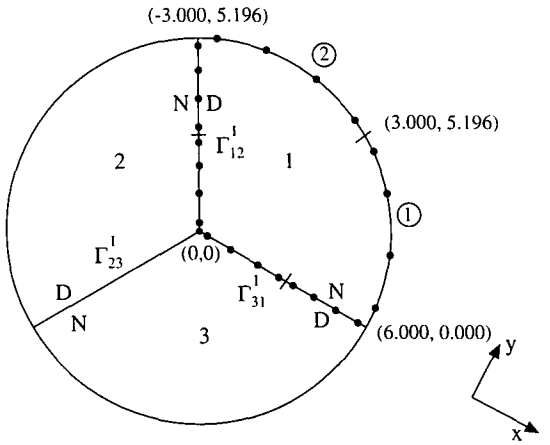

FIG. 9. The "Mercedes" star: discretization and matching interfacial conditions.

that the level of discretization is sufficiently accurate for the given problem.

In order to use the method for problems which require very fine discretization the stability of the assembled matrix has to be examined. For that purpose, the condition number of the assembled coefficient matrix in BEM for this problem is computed and plotted as a function of the number of collocation nodes.

It is clear from Fig. 8 that as the number of nodes increases, the condition number of the matrix also increases. However, for the same number of nodes used, the condition number of the matrix for non-conforming elements is lower than that of conforming elements. This suggests that the stability of the system is not sacrificed by the non-conformal placement of the nodes. The maximum number of nodes examined in this study is 768, which represents a fairly large boundary element mesh. If the condition number becomes prohibitively large then the problem can be solved using domain decomposition techniques with a lesser number of elements in each subdomain.

Case 2: Geometric Singularity due to Domain Partitioning

Bialecki *et al.* [28] used the "Mercedes star" problem to illustrate the use of hypersingular equations in BEM with three sub-domains. We use the same problem to test the numerical method developed here. The geometry of the domain is shown in Fig. 9. In all the three sub-domains, the Laplace equation (heat conduction with unit thermal conductivity) is solved with matching interfacial conditions. Six cubic non-conforming elements are used to discretize each domain. As mentioned before, we use the isoparametric representation to describe the geometry of the domain. For the given boundary discretization this does not introduce significant error in describing the perimeter as seen from Table IV. For comparing the numerical results, the harmonic function,

$$u = x^3 - 3xy^2, \tag{22}$$

is taken as the boundary condition. Dirichlet boundary conditions are imposed on the external boundary. For this sub-domain problem, boundary conditions on the common boundaries are arbitrarily specified initially and iterated until the converged solution is obtained. On one side of a common boundary, say, for example, Γ^I_{12}, Dirichlet boundary condition is imposed for sub-domain 1 to start the iterations. On the other side of the same boundary the Neumann condition is imposed for sub-domain 2. This way of assigning the boundary conditions is called the alternating D-N conditions and has been used successfully in the iterative solution of domain decomposition problems [29]. The boundary conditions for Γ^I_{23} and Γ^I_{31} are imposed in a similar manner. For each iteration, the potential and the normal gradient are updated as

$$T^{(n)} = (1 - \theta)T^{(p)} + \theta T^{(c)}, \tag{23}$$

where T is the dependent variable (potential or the flux), θ is

TABLE IV

Isoparametric and Actual Values of the End Points of Elements 1 and 2 in Fig. 9

Element	(x, y) computed	(x, y) actual
1	(5.996, 0.002)	(6.000, 0.000)
	(2.996, 5.194)	(3.000, 5.196)
2	(2.999, 5.192)	(3.000, 5.196)
	(−2.999, 5.192)	(−3.000, 5.196)

TABLE V

Mercedes Star Problem: Comparison of the Numerical Solution with Exact Analytical Solution along the Interface Γ_{12}'.

		Potential		Gradient	
x	y	Numerical	Analytical	Numerical	Analytical
−2.896	5.016	194.011	194.285	0.0029	0.0000
−2.505	4.339	125.810	125.752	0.0004	0.0000
−1.995	3.455	63.576	63.521	0.0005	0.0000
−1.604	2.778	33.045	33.021	−0.0002	0.0000
−1.396	2.418	21.778	21.760	0.0003	0.0000
−1.005	1.741	8.125	8.121	0.0000	0.0000
−0.495	0.857	0.966	0.970	0.0000	0.0000
−0.104	0.180	0.002	0.009	−0.0003	0.0000

the relaxation factor, (n) is the value at the next iteration, (p) is the value at the previous iteration, and (c) is the calculated value at the current iteration. Thus the procedure is an iterative method involving solution of one sub-domain at a time. Detailed discussion of the sub-domain iterative procedure is not presented here as this is not the theme of the paper. The converged results are shown in Table V. The value of the potential and the associated flux when projected to the point of singularity, i.e., (0, 0) is −0.0077 and −0.0005, respectively. This is very close when compared to the exact solution of 0.0 and 0.0 and is accurate by orders of magnitude to the solution obtained by the hypersingular equation method [28].

Case 3: Singularity Due to Boundary Condition

Non-conforming elements can be successfully used in solving problems with singularities arising due to boundary conditions. As an example, the problem of linear diffusion reaction in a catalyst particle is solved with mixed boundary conditions on one side of the particle. This problem has been solved before by many researchers and has been a benchmark in testing out new numerical techniques [30, 31, 17]. The geometry of the problem along with the boundary conditions is illustrated in Fig. 10. The governing differential equation is given by Eq. (7)

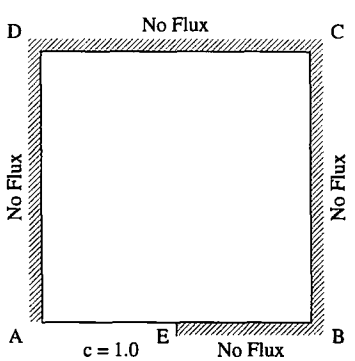

FIG. 10. Singularity at node E due to mixed boundary conditions for the diffusion–reaction problem.

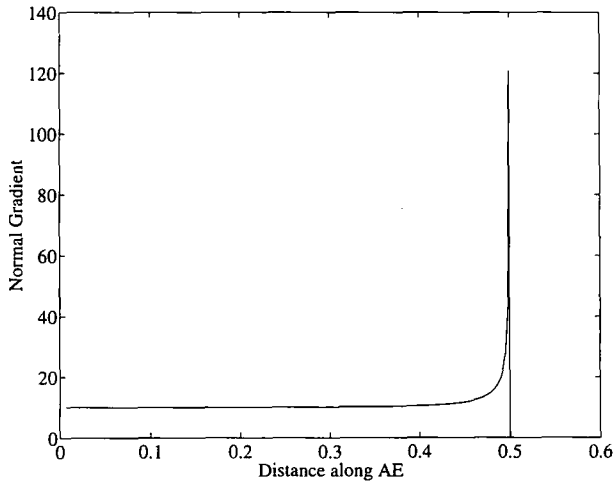

FIG. 11. The discontinuity of the normal gradient at point E; five cubic elements were used along AE and EB.

with $n = 1$. A value of $\phi = 10$ (which means steep concentration profiles) is used in this simulation. Regular BEM is used to solve this problem with special fundamental solution (Eq. (8)) as explained in Section 2. Ramachandran [17] has illustrated the use of special elements in the vicinity of the singularity to obtain accurate solution. The use of non-conforming elements obviates all the difficulties involved in tackling such problems without any loss in accuracy. Sixteen cubic elements are used to discretize the boundary, with eight of them in the vicinity of the singular point. Fig. 11 shows the normal gradient profile along the side AE. Note that the normal gradient at the point E is not defined and the use of non-conforming elements effectively eliminates the need to compute the gradient at that point.

6. ILLUSTRATION OF THE *rh* METHOD

As an example, the problem of boundary condition singularity (Case 3) is solved with *rh* mesh refinement to illustrate the methodology. As discussed earlier, the point E in Fig. 10 represents a case of singularity where the normal gradient is not defined.

To represent the variation of the normal gradient along the line segment AE, the mesh has to be finely graded near the singular point, E. Figure 12 shows the step wise grading of the mesh along AE, in conjunction with the result obtained by the procedure discussed in Section 4 and the improvement of the solution is illustrated in Fig. 13. Notice that the error indicator ε is initially high (0.18) when only one element is used. As the first refinement is made and the element AE is broken into two elements of 0.4 and 0.1 lengths (larger element towards A), ε drops to 0.006 in the larger element (which is farther from the singularity) and 0.071 in the smaller element. Since we had set an arbitrary tolerance of 0.015 for the refinement process to stop, the smaller element alone is refined into two

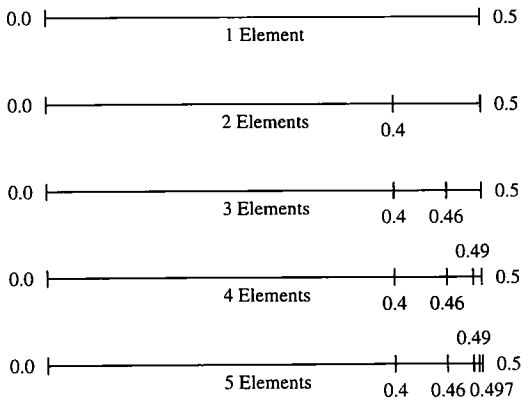

FIG. 12. The "*rh*" mesh refinement of the side *AE* in Fig. 10.

elements of 0.06 and 0.04 lengths each. Again, ε drops dramatically in the broken element farther from the singularity. This procedure is repeated until ε is within the set tolerance in all the elements. The effectiveness factor, η, defined as

$$\eta = \frac{1}{\Omega\phi^2}\int_\Gamma p\, d\Gamma, \tag{24}$$

is an important design parameter in catalysis. Here, Ω is the area of the object considered, Γ is the enclosing boundary, and p is the normal concentration gradient. As the mesh is refined, it can be seen from Fig. 13 that the effectiveness factor converges to the solution obtained by other methods in the literature [31, 17].

7. NON-LINEAR PROBLEMS

Non-conforming elements can also be used in the DRM for solving non-homogeneous and non-linear problems. A brief description of DRM was provided in Section 2. Here, we solve the case study 3 again, to test the accuracy of non-conforming elements in DRM. First the linear problem ($n = 1$ in Eq. (7)) is solved with only two boundary elements along *AE* (the second configuration in Fig. (12)). Thirty internal nodes are placed (mostly near the singularity). The effectiveness factor η as defined in Eq. (24) is calculated to be 0.05466. This is very close to the result shown in stage 2 of Fig. 13. Now the same concept can be extended to non-linear problems as well. For example, when we consider $n = 2$ in Eq. (7), we obtain an effectiveness factor of 0.04549. The use of non-conforming elements in DRM is not restricted in solving the non-linearities in reaction rate alone. Particularly for convection–diffusion–reaction problems and sub-domain DRM problems, the technique developed here could be of great use.

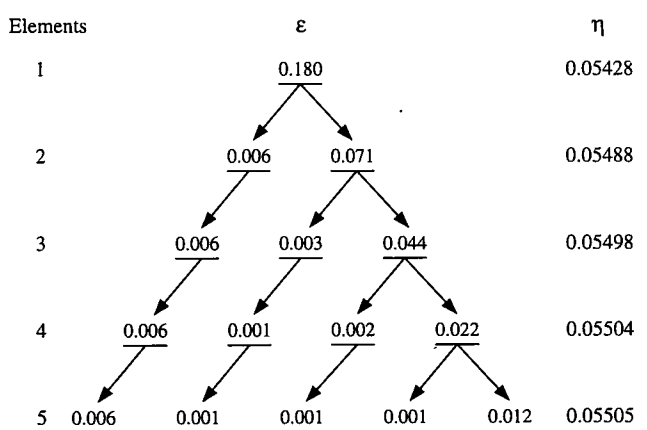

FIG. 13. The error indicator ε for each element along *AE* in Fig. 10.

8. CONCLUSION

In this paper, it is shown that the singularities arising due to the geometry and boundary conditions in Laplace and Poisson type problems can be successfully handled by using non-conforming boundary elements. A systematic basis for the choice of the collocation points is provided. The D-D and D-N singularities are circumvented without any special treatment. The accuracy of the method is demonstrated for both regular and sub-domain BEM as well as DRM. The amount of book-keeping in sub-domain BEM is reduced by using non-conforming elements. The option to change the placement of the collocation points with a change in the parameters α and β results in the generation of two (or more) solutions for the same level of discretization. This in turn is used in the error estimation studies. Disadvantages of non-conforming elements indicated in the literature are not seen from our computation. We believe that the method has potential in 3D simulation for problems in heat transfer and fluid mechanics.

REFERENCES

1. C. A. Brebbia, L. C. Wrobel, and J. C. F. Telles, *Boundary Element Techniques* (Springer-Verlag, Berlin, 1984).
2. P. K. Banerjee, *Boundary Element Methods in Engineering* (McGraw–Hill, New York, 1994).
3. A. K. Mitra and M. S. Ingber, *Int. J. Numer. Methods Eng.* **36,** 1735 (1993).
4. S. P. Walker and R. T. Fenner, *Int. J. Numer. Methods Eng.* **28,** 2569 (1989).
5. A. J. Kassab and R. S. Nordlund, *Commun. Numer. Methods Eng.* **10,** 385 (1994).
6. M. A. Jaswon and G. T. Symm, *Integral Equation Methods in Potential Theory and Elastostatics* (Academic Press, New York, 1977).
7. Ramachandran, P. A., *Boundary Element Methods in Transport Phenomena* (Computational Mechanics/Elsevier, Southampton, NY, 1994).
8. G. D. Manolis and P. K. Banerjee, *Int. J. Numer. Methods Eng.* **23,** 1885 (1986).
9. C. A. Brebbia and S. M. Niku, *Int. J. Numer. Methods Eng.* **25,** 283 (1988).
10. C. A. Brebbia and R. Magureanu, *Eng. Anal.* **4,** 178 (1987).
11. Guiggiani, M., *Int. J. Numer. Methods Eng.* **29,** 1247 (1990).
12. B. Szabó and I. Babuška, *Finite Element Analysis* (Wiley, New York, 1989).
13. C. A. Brebbia and D. Nardini, *Int. J. Soil Dyn. Earthquake Eng.* **2,** 228 (1983).

14. C. A. Brebbia and J. Dominguez, *Boundary Elements—An Introductory Course* (Computational Mechanics/McGraw–Hill, New York, 1989).
15. P. W. Partridge, C. A. Brebbia, and L. C. Wrobel, *The Dual Reciprocity Boundary Element Method* (Computational Mech., Southampton, NY, 1992).
16. S. R. Karur and P. A. Ramachandran, *Boundary Elements Commun.* **6,** 55 (1995).
17. P. A. Ramachandran, *Chem. Eng. J.* **47,** 169 (1991).
18. J. Villadsen and M. L. Michelsen, *Solution to Differential Equation Modeling by Polynomial Approximation* (Prentice–Hall, New York, 1978).
19. P. Beckmann, *Orthogonal Polynomials for Engineers and Physicists* (Golem, Boulder, CO, 1973).
20. G. Szego, *Orthogonal Polynomials* (Amer. Math. Soc., New York, 1959).
21. C. D. Holland and A. I. Liapis, *Computer Method for Solving Dynamic Separation Problems* (McGraw–Hill, New York, 1983).
22. J. A. Ligget and J. R. Salmon, *Int. J. Numer. Methods Eng.* **17,** 543 (1981).
23. G. Chen and J. Zhou, *Boundary Element Methods* (Academic Press, San Diego, 1992).
24. D. N. Arnold and W. L. Wendland, *Math. Comput.* **41,** 349 (1983).
25. M. Costabel and E. P. Stephan, *Math. Comput.* **49,** 461 (1987).
26. J. Saranen, *Numer Math.* **53,** 499 (1988).
27. Y. Yan, *Math. Comput.* **54,** 139 (1990).
28. R. Bialecki, R. Dallner, and G. Kunn, *Comput. Methods Appl. Mech. Eng.* **103,** 399 (1993).
29. D. Funaro, A. Quarteroni, and P. Zanolli, *SIAM J. Numer. Anal.* **25,** 1213 (1988).
30. P. L. Mills and M. P. Duduković, *Ind. Eng. Chem. Fundam.* **18,** 139 (1979).
31. P. L. Mills, S. Lai, M. P. Duduković, and P. A. Ramachandran, *Comput. Chem. Eng.* **12,** 37 (1988).